# Parametrically polarization-shaped pulses via a hollow-core photonic crystal fiber

Fabian Weise,* Georg Achazi, and Albrecht Lindinger
*Institut für Experimentalphysik, Freie Universität Berlin, Arnimallee 14, D-14195 Berlin, Germany*
(Received 30 March 2010; revised manuscript received 10 September 2010; published 24 November 2010)

We present a procedure to generate parametrically shaped pulses after propagation through a microstructured hollow-core photonic crystal fiber. The properties of the fiber are characterized and employed to analytically design sequences of subpulses which are available after the fiber. In these sequences, each subpulse can be individually controlled in its physically intuitive parameters: position in time, energy, phase, and chirp as well as the polarization state with orientation, ellipticity, and helicity. Various endoscopic applications may arise from this approach.

DOI: 10.1103/PhysRevA.82.053827 PACS number(s): 42.25.Ja, 82.50.Nd, 42.79.Kr, 42.81.Gs

## I. INTRODUCTION

Femtosecond laser pulses have become a popular tool in science and technology. Their application ranges from fundamental research of quantum dynamics to material processing and medical applications. For many of these applications, it could be desirable to transport the pulses using fiber optics. Conventional fibers which guide the light by total internal reflection can only be used to a limited extent for pulses because of constraints of the core material. Chromatic dispersion strongly broadens the pulses temporally. This could be overcome by prechirping the pulses using prism and grating compressors or adaptive phase control [1]. However, the transmission of ultrashort pulses is limited to pulse energies below 0.1 nJ because nonlinear effects such as self-phase modulation become significant. This makes standard fibers unsuitable for many applications. The use of two-dimensional microstructures revolutionized fiber optics. The guiding mechanism in such photonic crystal fibers is fundamentally different compared to standard fibers. It relies on a photonic band gap waveguide [2]. The properties of these fibers are determined by the geometry of the structure and its dimensions. Hollow-core photonic crystal fibers are particularly suitable to transport short laser pulses which have a high peak intensity since in this type of fiber, the major fraction of the pulse's intensity propagates in the air-filled hollow core. This allows for increasing the transmitted pulse energy by at least 2 orders of magnitude. In these fibers, the attenuation is very low, and the dispersion curve is nearly flat for a broad band of frequencies. The accessible pulse energy is suitable to drive multiphoton processes and extends the area of applications.

Shaping of femtosecond laser pulses allows their adaptation to a specific quantum system and control of the final state of the excitation pathway. For complex systems, the optimal pulse shape is often found in closed-feedback-loop optimizations in which an observable of the desired state serves as a feedback signal [3]. This technique of coherent control has been successfully applied in the investigation and in the control of reaction mechanisms of various fields [4]. Including the polarization increased the controllability of the electric field and propelled the development of new pulse-shaping setups [5–8].

The optimal pulses found in feedback loop optimizations are often very complex. Encoding the pulses with a small number of parameters restricts the search space, results in faster convergence, and the obtained pulses are easier to interpret. Moreover, this allows for systematic analysis of the particular quantum system [9–11]. So far, pulse shaping in combination with optical fibers was only used for compensating for the group velocity dispersion [1,12,13] and polarization mode dispersion [14] or for controlling the supercontinuum generation [15,16].

In this article, we introduce a procedure to generate ultrashort pulses which are parametrically shaped in phase, amplitude, and polarization after propagation through a hollow-core photonic crystal fiber. Pulses which propagate through an optical fiber are distorted because of the dispersion, birefringence, and nonlinear effects of the fiber. These properties of the fiber are investigated and taken into account in the pulse-shaping procedure in order to obtain the desired pulse shape after transmission through the fiber. The generated pulses are parameterized in a sequence of subpulses. In this sequence, the physically intuitive parameters of each subpulse—energy, position in time, phase, and chirps as well as the polarization with ellipticity and orientation—can be individually set.

## II. EXPERIMENTAL SETUP

A schematic of the experimental setup is depicted in Fig. 1. The laser pulses are generated by an oscillator (Mira, Coherent) having a pulse energy of 9 nJ at a repetition rate of 76 MHz. For the analysis of nonlinear effects and to investigate the intensity limit of the pulse-shaping procedure, the pulses can be amplified up to 3.3 $\mu$J pulse energy using a regenerative amplifier (RegA 9050, Coherent) having a repetition rate of 250 kHz. The spectral width amounts to 22 nm (full width at half maximum) at a central wave length of 805 nm. These pulses are modulated by a pulse shaper which is similar to the shaper setup presented in [6]. It consists of a $4f$-line with cylindrical lenses of $f = 200$ mm and gratings of 1200 grooves/mm. Two standard double liquid crystal modulators (SLM-256 and SLM-640, CRi) with the optical axis oriented at $\pm 45^\circ$ are placed in the Fourier plane separated by a horizontally oriented polarizer. This setup is capable of modulating the phase, amplitude, and polarization simultaneously and independently. The polarization control is restricted to pulses with a fixed horizontal or vertical orientation of the principal axis of the electric field ellipse. This restriction is not obstructive since horizontal and vertical

*weise@physik.fu-berlin.de

 

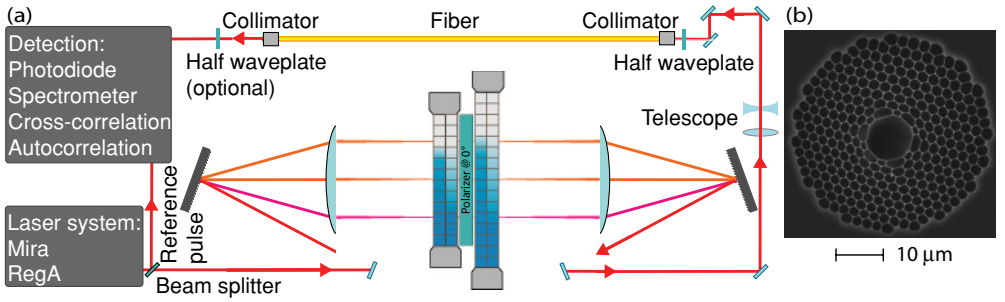


FIG. 1. (Color online) (a) Experimental setup. The ultrashort laser pulses are shaped in phase, amplitude, and polarization by two double liquid crystal modulators situated in the Fourier plane of a $4f$-line. The pulses are coupled into a photonic-crystal hollow-core fiber with the help of a telescope and a collimator. After propagation through the fiber, the pulses are characterized using autocorrelation and cross-correlation measurements. (b) A micrograph of the fiber (from [17]).

polarizations are sufficient to generate all polarization states after the fiber.

The shaped pulses are coupled to the fiber using a telescope and a standard collimator. A half-wave plate placed before the fiber is used to rotate the polarization of the incident pulse respective to the fiber. The fiber used is a microstructured single-mode hollow-core fiber (HC-800-01, NKT Photonics) measuring 110 cm in length. More than 95% of the transmitted light is guided through the hollow core surrounded by a structure of 12 hollow hexagons of silica [cf. Fig. 1(b)]. The cross-sectional area of the core of this particular fiber measures 9.2 $\mu$m for the short axis and 9.5 $\mu$m for the long axis. Owing to this asymmetry, the fiber is birefringent, having two optical axes denoted as fast ($f$) and slow ($s$). In these measurements, the slow axis of the end of the fiber is rotated by $-60^\circ$ respective to the horizontal axis of the laboratory frame. The ends of the fiber are spliced onto thin glass windows of 100 $\mu$m thickness and are connectorized by PC-FC plugs. The fiber is transparent for a broad band of wavelengths (>70 nm) centered at 830 nm. In this range, the dispersion curve is nearly flat, whereas the zero-dispersion wavelength is located at 805 nm.

After propagation through the fiber, the pulses are characterized. For simple single pulses, the pulse duration is determined by autocorrelation measurements. In case of complex polarization-shaped pulses, the pulse shape is obtained by time-resolved ellipsometry. In this procedure, the cross-correlation traces in 10 different orientations covering 180° are measured, and the ellipse of the electric field is retrieved for every time step. These data are summarized in a graph which shows the time-dependent intensity (red curve) and polarization state including orientation (dotted blue) and ellipticity (dashed green), as depicted in Figs. 2 and 3. The ellipicity ($r$) is defined as the ratio of the minor to the major axis of the electric field ellipse. On the basis of these data, the three-dimensional shape of the pulse is calculated [7].

## III. PULSES GUIDED BY THE HOLLOW-CORE PHOTONIC CRYSTAL FIBER

First, we are using the pulses from the oscillator having a maximum energy of 0.24 nJ after transmission through the fiber. The spectrum of a short pulse which propagated through the optical fiber is unchanged compared to the spectrum before the fiber. This means that nonlinear effects, such as self-phase modulation, do not occur and the fiber can be treated as a linear element. In this case, the modulation of the pulse induced by the fiber can generally be described by a product of the Jones matrix of the fiber $\tilde{\mathbf{F}}$ and the vector of the incoming electric field $\tilde{\mathbf{E}}_{\text{in}}$ [Eq. (1)]:

$$\tilde{\mathbf{E}}_{\text{out}} = \tilde{\mathbf{F}} \cdot \tilde{\mathbf{E}}_{\text{in}} \;\Leftrightarrow\; \tilde{\mathbf{E}}_{\text{in}} = \tilde{\mathbf{F}}^{-1} \cdot \tilde{\mathbf{E}}_{\text{out}}. \tag{1}$$

If the Jones matrix of the fiber is known, it can be inverted and applied to the desired electric field after the fiber $\tilde{\mathbf{E}}_{\text{out}}$ to calculate the required incoming field [Eq. (1)]. This electric field can be generated by a suitable pulse shaper.

### A. Characterization of the fiber

In order to provide a more conceptional method for the generation of parametrically shaped pulse sequences, the effect of the fiber on the transmitted pulse is further investigated. A short pulse is coupled to the fiber being linearly polarized, oriented at 45° relative to the fast and slow axes of the fiber. The time evolution of the pulse after propagation through the fiber is depicted in Fig. 2(a). The intensity curve exhibits two pulses separated by 1.16 ps. Both subpulses are linearly polarized and perpendicularly oriented along the optical axes of the fiber. The temporal splitting is denoted as difference group delay and is induced by the strong birefringence of the fiber. The asymmetric shape in time is characteristic for a cubic spectral phase of the fiber's dispersion curve. When the incoming pulse is oriented along the fast (slow) axis of the fiber, the intensity evolution of the transmitted pulse shows only a single pulse at earlier (later) times.

For pulses which are only polarized in one plane, the generation of intended pulse shapes after the fiber is straightforward. The desired pulse shape is written on the modulator superimposed with an additional phase function which compensates for the dispersion of the fiber along the respective axis. This linearly polarized pulse is coupled to the fiber oriented parallel to one axis of the fiber, propagates in the fiber, and leaves the fiber with the desired shape linearly polarized along the same axis of the fiber.

In case of polarization-shaped pulses, the vectorial electric field has to be considered. The polarization state is determined by the relative amplitude along two perpendicular axes and the relative phase between these components. This can be directly employed for constructing parametrically shaped pulses after

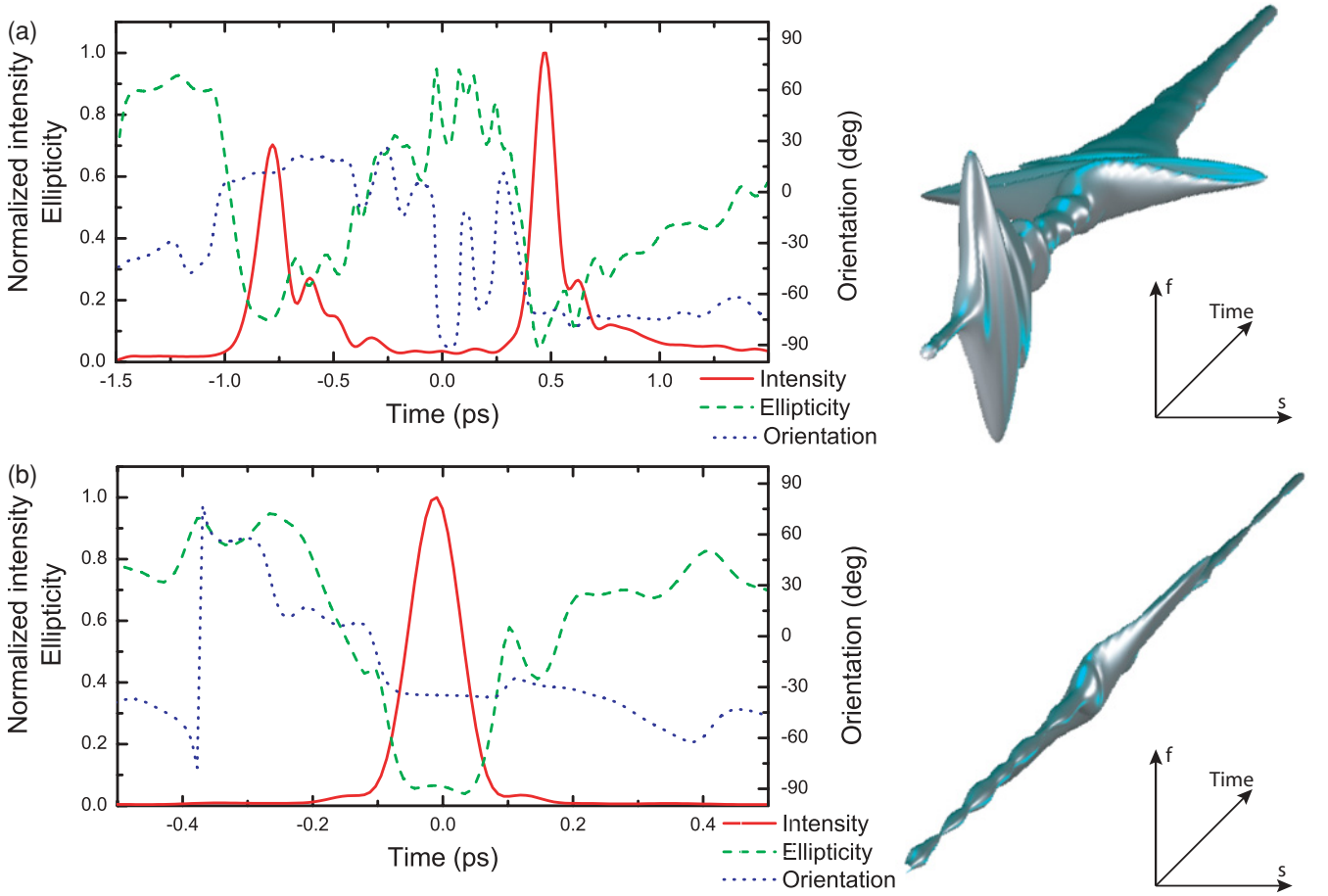


FIG. 2. (Color online) Pulses after transmission through the fiber. (a) A linearly polarized short pulse enters the fiber oriented at 45° to the optical axis of the fiber. (b) A pair of compensated orthogonally polarized pulses with a difference phase of zero produces a single linearly polarized pulse oriented at +45° respective to the axes of the fibers.

propagation through the fiber. The pulse shaper produces an orthogonal, linearly polarized pulse pair which is polarized along the fast and the slow axes of the fiber. The power of the two transmitted pulses has to be equal. This can be adjusted by the compensation parameters $A_c^s$ and $A_c^f$, which are, in this case, set to 1. For each pulse, the chirp is adapted separately in order to obtain a short pulse after the propagation through the fiber. Furthermore, a linear phase function is employed to shift the pulses in time to achieve temporal overlap. The temporal shape of the pulses needs to be identical, and the temporal overlap must be precisely set.

This adjustment is very tedious. Therefore the spectral phase function is found in a feedback loop optimization using an evolutionary algorithm. In this procedure, the Taylor terms of the spectral phase $\Phi_c^{s,f}(\omega)$ for the compensation of the dispersion along the fast and slow axis of the fiber are optimized up to the fourth order. The power of the transmitted pulse after a polarizer oriented at 45° respective to the optical axes of the fiber serves as a feedback signal. In the maximization, the Taylor terms are found to be $b_0^s = -0.25\,\pi$, $b_1^s = -400$ fs, $b_2^s = -7000$ fs$^2$, $b_3^s = -7.30 \times 10^5$ fs$^3$, $b_4^s = -5.50 \times 10^6$ fs$^4$ for the slow axis and $b_0^f = 0$, $b_1^f = +766$ fs, $b_2^f = +8827$ fs$^2$, $b_3^f = -3.90 \times 10^5$ fs$^3$, $b_4^f = +2.48 \times 10^6$ fs$^4$ for the fast axis. Mechanical stress in the fiber induced by bending or twisting as well as changes in temperature results in slightly different compensation terms for the fast and slow axes. In particular, the state of polarization is sensitive to these changes. An active adaption of the compensation parameters could account for this issue in an application. These spectral phase parameters serve as an offset for the fast and slow pulses, respectively.

### B. Control of single pulses

Having this compensation applied, the pulses which are transmitted through the fiber interfere with a single short pulse which is linearly polarized at +45° respective to the optical axis of the fiber, as depicted in Fig. 2(b). This pulse can be arbitrarily controlled in phase, amplitude, and polarization. By changing the amplitudes of the fast and slow pulses $f_N$ and $s_N$, the orientation of the pulse can be changed. The shift of the relative phase $\epsilon_N$ between the fast and slow components results in a change in ellipticity. Adding a desired spectral phase $\phi_N(\omega)$ to the compensation parameters controls the shape and the position in time of the shaped pulse.

### C. Generation of parametric pulse sequences

This procedure can be extended to pulse sequences consisting of $N$ subpulses. Any individual subpulse consists of

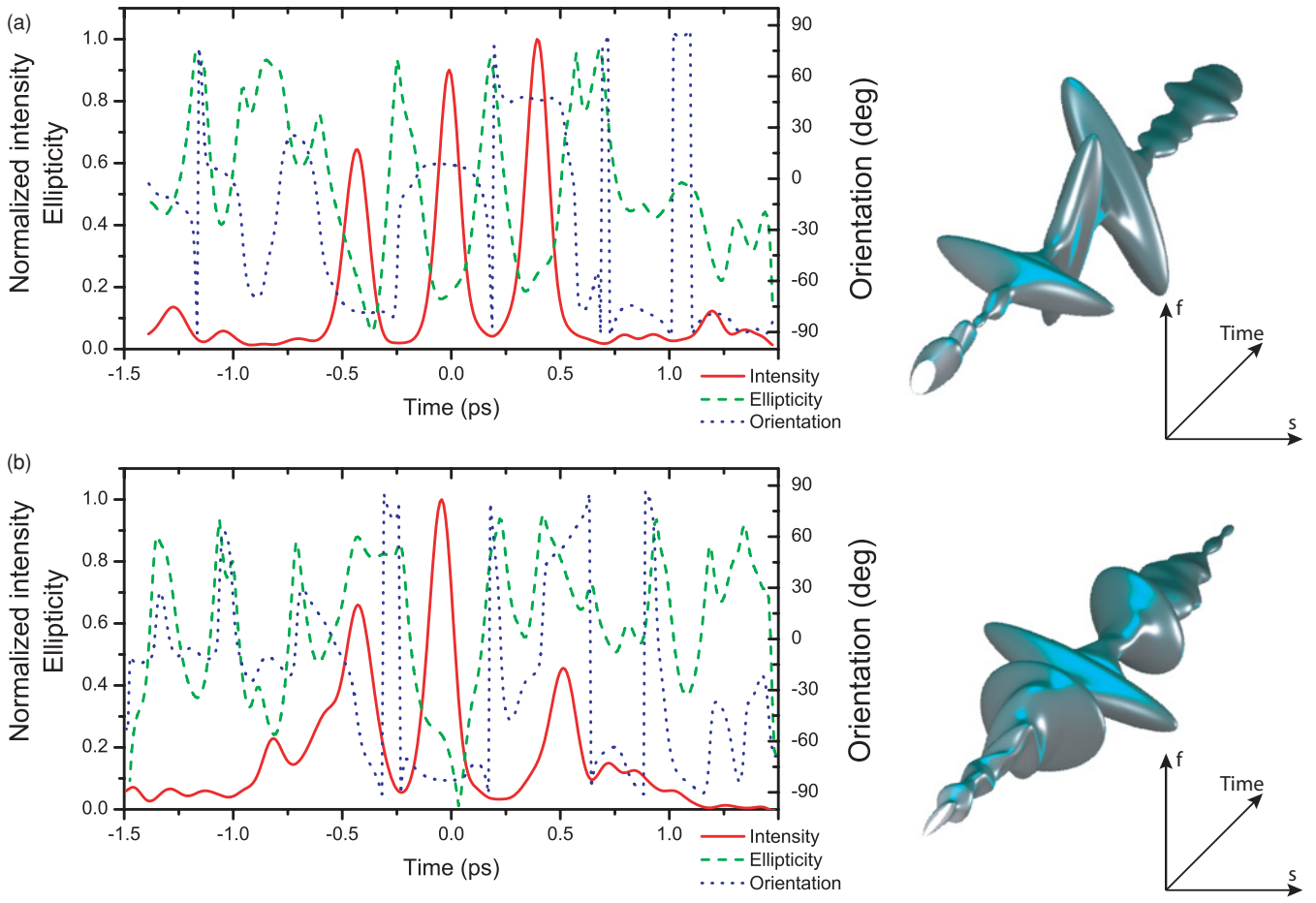


FIG. 3. (Color online) Complex amplified polarization-shaped pulse sequences after propagation through the hollow-core fiber. The time-dependent polarization and intensity are accompanied by a three-dimensional representation of the pulse.

two prototype pulses whose energy ratio, relative phase, delay, and chirp is set and the respective compensation is added. The electric field of the parameterized sequence is expressed as the superposition of $N$ subpulses:

$$\tilde{\mathbf{E}}(\omega) = \tilde{E}_{\text{in}}(\omega) \sum_N \begin{pmatrix} A_c^s s_N e^{i[\Phi_c^s(\omega)+\phi_N(\omega)+\epsilon_N]} \\ A_c^f f_N e^{i[\Phi_c^f(\omega)+\phi_N(\omega)]} \end{pmatrix}. \quad (2)$$

The polarization state of the subpulses which is described by the orientation ($\gamma$) and the ellipticity ($r$) is transformed to the relative phase ($\epsilon$) and the spectral amplitude ($f_N$ and $s_N$) of the electric field by the following equations:

$$s_N = \sqrt{\frac{1}{2} I_N \left(1 + \frac{r_N^2 - 1}{r_N^2 + 1} \cos(2\gamma_N)\right)}, \quad (3)$$

$$f_N = \sqrt{\frac{1}{2} I_N \left(1 - \frac{r_N^2 - 1}{r_N^2 + 1} \cos(2\gamma_N)\right)}, \quad (4)$$

$$\epsilon_N = \pm \arccos\left(\sqrt{\frac{(r_N^2 - 1)^2}{1 + r_N^4 + r_N^2[\cot^2(\gamma_N) + \tan^2(\gamma_N)]}}\right). \quad (5)$$

The intensity of the subpulse is described by $I_N$, and the sign of the relative phase determines the helicity of the electric field. The general pulse sequence of $N$ arbitrarily shaped subpulses after the fiber requires $2 \times N$ linearly polarized subpulses to enter the fiber.

In Fig. 3(a), a sequence of three linearly polarized subpulses separated by 400 fs is shown. The orientations of the subpulses are set to 0°, 90°, and −45° relative to the slow axis of the fiber. In the second example, which is depicted in Fig. 3(b), the variation of the distance in time, ellipticity, subpulse energy, and chirps is presented. The sequence consists of three subpulses which are separated by 300 and 500 fs. The first and the last subpulse are circularly polarized. Both are quadratically chirped by $\pm 8 \times 10^5$ fs$^2$, wherein the sign determines the direction of the pulse's temporal asymmetry. The second pulse is linearly polarized along the slow axis of the fiber and is unchirped. The energy of the first and last subpulse is set 2 times larger than of the central pulse.

## IV. INVESTIGATION OF NONLINEARITIES

The onset of nonlinear effects limits the pulse energy which can be transmitted through the fiber. The intensity dependence is investigated by using amplified pulses which reach a maximum pulse energy of 72 nJ after transmission through the fiber.

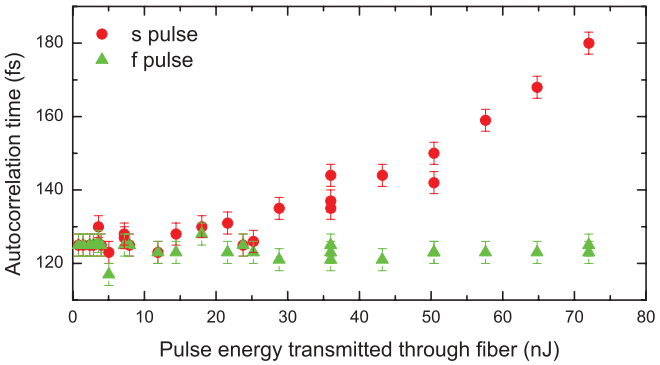


FIG. 4. (Color online) Investigation of nonlinearities. The autocorrelation time is measured in dependence of the pulse energy for two linearly polarized pulses.

The pulse duration determined by the autocorrelation time serves as an indicator for the appearence of nonlinear effects. This measurement was carried out for two linearly polarized single pulses which were oriented parallel to the fast and the slow axis of the fiber. The energy-dependent autocorrelation times are presented in Fig. 4. For the pulse oriented along the fast axis of the fiber, the pulse duration is not sensitive to the power in the considered range. In contrast to this, the duration of the slow pulse varies strongly by the pulse energy. For pulse energies of up to 24 nJ, the pulse duration is equal within the errors. The increase in the pulse length can be directly attributed to nonlinear effects. These nonlinearities cannot be analytically compensated by precalculation of correction functions and limit the capabilities of the predetermined parametric pulse shaping. For this reason, the upper limit of the subpulse energy is set to 24 nJ for pulses of about 90 fs. A pulse consisting of several separated subpulses can have a larger total energy. This is demonstrated in the example pulses in Fig. 3 using pulses from the amplifier. The total pulse energy of the transmitted complex shaped pulses amounts to about 24 nJ and 30 nJ, respectively. Here the maximum pulse energy is limited by the used amplifier. However, when only considering subpulses which are linearly polarized along the fast axis of the fiber, each subpulse can exceed the energy of 72 nJ, resulting in shaped pulses with a large overall pulse energy which agrees with [18].

## V. CONCLUSION AND OUTLOOK

In summary, we presented a method to generate arbitrarily shaped femtosecond laser pulses after propagation through a microstructured hollow-core photonic crystal fiber which is suitable for transmitting pulses of high energy. We analyzed the properties of the fiber such as dispersion, birefringence, and the onset of nonlinearities. Moreover, a parametrization of subpulse sequences, including a compensation of the modulation induced by the fiber, was introduced which is particularly suited for birefringent fibers. In this procedure, each subpulse can be controlled individually and independently in its physically intuitive parameters position in time, energy, phase, chirps, and the state of polarization with orientation, ellipticity, and helicity. This analytical method was exemplified with two complexly shaped multipulse sequences. Extending this method of predetermined pulse generation to the nonlinear regime could facilitate the broadened frequency spectrum and self-compression. The development of these techniques provides the possibility to bring custom-tailored ultrashort laser pulses to locations which are not accessible by an open beam. This extends the area of application of coherent control. In particular, biophysics and medicine would benefit from endoscopic in vivo application of shaped femtosecond laser pulses for multiphoton microscopy, spectroscopy, or photodynamic therapy [19–21]. Furthermore, the highly confined light field at the end of the fiber can be employed in near-field microscopy with nanometer spatial and femtosecond temporal resolution [22].

## ACKNOWLEDGMENTS

We thank Ludger Wöste and the Deutsche Forschungsgemeinschaft (SFB 450) for financial support.

[1] S. H. Lee, A. L. Cavalieri, D. M. Fritz, M. Myaing, and D. A. Reis, Opt. Lett. **29**, 2602 (2004).
[2] P. Russell, Science **299**, 358 (2003).
[3] R. S. Judson and H. Rabitz, Phys. Rev. Lett. **68**, 1500 (1992).
[4] P. Nuernberger, G. Vogt, T. Brixner, and G. Gerber, Phys. Chem. Chem. Phys. **9**, 2470 (2007).
[5] T. Brixner, G. Krampert, T. Pfeifer, R. Selle, G. Gerber, M. Wollenhaupt, O. Graefe, C. Horn, D. Liese, and T. Baumert, Phys. Rev. Lett. **92**, 208301 (2004).
[6] M. Plewicki, S. M. Weber, F. Weise, and A. Lindinger, Appl. Phys. B **86**, 259 (2007).
[7] M. Plewicki, F. Weise, S. M. Weber, and A. Lindinger, Appl. Opt. **45**, 8356 (2006).
[8] F. Weise and A. Lindinger, Opt. Lett. **34**, 1258 (2009).
[9] S. M. Weber, M. Plewicki, F. Weise, and A. Lindinger, J. Chem. Phys. **128**, 174306 (2008).
[10] F. Dimler, S. Fechner, A. Rodenberg, T. Brixner, and D. J. Tannor, New J. Phys. **11**, 105052 (2009).
[11] F. Weise and A. Lindinger, Appl. Phys. B **101**, 79 (2010).
[12] C.-C. Chang, H. P. Sardesai, and A. M. Weiner, Opt. Lett. **23**, 283 (1998).
[13] Z. Jiang, S.-D. Yang, D. E. Leaird, and A. M. Weiner, Opt. Lett. **30**, 1449 (2005).
[14] H. Miao, A. M. Weiner, L. Mirkin, and P. J. Miller, Opt. Lett. **32**, 2360 (2007).
[15] J. Tada, T. Kono, A. Suda, H. Mizuno, A. Miyawaki, K. Midorikawa, and F. Kannari, Appl. Opt. **46**, 3023 (2007).
[16] D. Lorenc, D. Velic, A. N. Markevitch, and R. J. Levis, Opt. Commun. **276**, 288 (2007).
[17] Data sheet: Hollow Core Photonic Bandgap Fiber HC-800-01, NKT Photonics.

[18] A. A. Ishaaya, C. J. Hensley, B. Shim, S. Schrauth, K. W. Koch, and A. L. Gaeta, Opt. Express **17**, 18630 (2009).
[19] M. T. Myaing, D. J. MacDonald, and X. Li, Opt. Lett. **31**, 1076 (2006).
[20] K. König, J. Microsc. **200**, 83 (2000).
[21] K. T. Tsen, S.-W. D. Tsen, C.-L. Chang, C.-F. Hung, T.-C. Wu, and J. G. Kiang, J. Phys.: Condens. Matter **19**, 322102 (2007).
[22] B. A. Nechay, U. Siegner, M. Achermann, H. Bielefeldt, and U. Keller, Rev. Sci. Instrum. **70**, 2758 (1999).